Oncogene (2011) 30, 1551–1565

www.nature.com/onc

ORIGINAL ARTICLE

Genome-wide shRNA screen reveals increased mitochondrial dependence upon mTORC2 addiction

M Colombi[1,4], KD Molle[1,4], D Benjamin[1,4], K Rattenbacher-Kiser[2], C Schaefer[2], C Betz[1], A Thiemeyer[1], U Regenass[3], MN Hall[1] and C Moroni[1]

[1]*Biozentrum, University of Basel, Basel, Switzerland;* [2]*Institute of Medical Microbiology, University of Basel, Basel, Switzerland and* [3]*Actelion Pharmaceuticals Ltd, Allschwil, Switzerland*

Release from growth factor dependence and acquisition of signalling pathway addiction are critical steps in oncogenesis. To identify genes required on mammalian target of rapamycin (mTOR) addiction, we performed a genome-wide short hairpin RNA screen on a v-H-ras-transformed Pten-deficient cell line that displayed two alternative growth modes, interleukin (IL)-3-independent/mTOR-addicted proliferation (transformed growth mode) and IL-3-dependent/mTOR-non-addicted proliferation (normal growth mode). We screened for genes required only in the absence of IL-3 and thus specifically for the transformed growth mode. The top 800 hits from this conditional lethal screen were analyzed *in silico* and 235 hits were subsequently rescreened in two additional Pten-deficient cell lines to generate a core set of 47 genes. Hits included genes encoding mTOR and the mTOR complex 2 (mTORC2) component rictor and several genes encoding mitochondrial functions including components of the respiratory chain, adenosine triphosphate synthase, the mitochondrial ribosome and mitochondrial fission factor. Small interfering RNA knockdown against a sizeable fraction of these genes triggered apoptosis in human cancer cell lines but not in normal fibroblasts. We conclude that mTORC2-addicted cells require mitochondrial functions that may be novel drug targets in human cancer.
Oncogene (2011) **30,** 1551–1565; doi:10.1038/onc.2010.539; published online 20 December 2010

Keywords: shRNA screen; mTOR addiction; IL-3 dependence; mitochondria; drug targets

Introduction

The identification of dominant oncogenes has raised hopes that the corresponding oncoproteins may be vulnerable points in cancer cells. This expectation has been partially fulfilled, particularly for oncoproteins with protein kinase activity, which allowed the development of targeted inhibitors with substantial clinical benefit (Thaimattam *et al.,* 2007; Muller, 2009; Pytel *et al.,* 2009). Conversely, clinical translation of efforts focused on currently 'non-druggable' oncoproteins, such as transcription factors or G-proteins, have been disappointing and any future progress will depend on further breakthroughs. As many oncoproteins are generally upstream components of signalling networks, a reasonable assumption is that the downstream components that ultimately execute a particular oncoprotein's requisite functions may similarly serve as drug targets, even if they are not mutated. Support for this concept is the demonstration that in tumor cells, the ras p21 protein becomes 'rewired' to the downstream kinase STK33, which in turn becomes a possible drug target (Scholl *et al.,* 2009). For such corresponding downstream genes, the term 'non-oncogenes' has been proposed (Solimini *et al.,* 2007). Although presumably only few oncogenes remain to be discovered, the identification of non-oncogenes as potential drug targets to reverse oncogenic progression is a new and promising area of investigation.

mTOR is a non-oncogene with a role in cancer (Guertin and Sabatini, 2007). mTOR is a conserved serine/threonine kinase that integrates signals from growth factors, nutrient supply and energy status to activate cell growth (Wullschleger *et al.,* 2006). It is found in two structurally and functionally distinct complexes termed mTOR complex 1 (mTORC1) and mTORC2. Activating mutations in mTOR in human cancer are apparently rare and have been reported, based on a database search, only recently (Sato *et al.,* 2010). Upstream negative regulators of mTOR including Pten, Tsc2, Tsc1 and LKB1 are well-known tumor suppressors and their loss activates mTOR (Chiang and Abraham, 2007). Thus, the mTOR pathway is a promising target for therapy, and the mTOR inhibitor rapamycin and its analogues show clinical promise.

Non-conventional screening systems are required to identify non-oncogenes involved in cancer. An important advance in the genetic analysis of human cancer has been the development of genomic short hairpin RNA (shRNA) libraries that permit interrogation of gene functions globally and systematically for their possible requirement in the oncogenic process (Moffat *et al.,* 2006). Arrayed formats of genome-scale libraries combined with robotic multiplate processing technology permits efficient high-throughput screens with cell-based

Correspondence: Professor MN Hall or Professor C Moroni, Biozentrum, University of Basel, Klingelbergstrass 70, Basel-Stadt, Basel CH-4056, Switzerland.
E-mail: christoph.moroni@unibas.ch and m.hall@unibas.ch
[4]These authors contributed equally to this work.
Received 1 May 2010; revised 13 September 2010; accepted 15 September 2010; published online 20 December 2010

assays. Pooled shRNA libraries have also been used, in which a barcode sequence tag allows retrospective identification of growth suppressing oligos, as these will be progressively diminished in a cell pool over time (Schlabach *et al.,* 2008). The incorporation of appropriate controls in the design of a particular screening strategy allows determination of whether a specific gene is required exclusively for oncogenic growth. This strategy has been pursued to reveal synthetic lethality between non-oncogenes and the prototypic Kras oncogene (Luo *et al.,* 2009).

In this study, we describe a conditional lethal shRNA-based screen to identify effector genes of oncogenicity. The approach exploits a Pten-deficient mutant cell line that is mTOR pathway addicted, but only in the absence of interleukin (IL)-3. We hence screened for genes that were required for growth and survival only in the absence of IL-3. We obtained a set of approximately 800 candidate genes that was reduced, on rescreening of the top 235 candidates in different Pten-deficient lines, to a core set of 47 genes. This core set contains several genes encoding mitochondrial functions in addition to other genes potentially important in oncogenesis. Targeted knockdown of 24 of the core set of 47 genes revealed 8 genes required for proliferation in two human cancer cell lines but not in normal fibroblasts, suggesting that these genes encode potential novel drug targets in human cancer.

Results

IL-3-sensitive mTOR addiction

We developed a cell system to screen by RNA interference for genes required specifically for a transformed growth mode. Central to this system is a murine Pten mutant (termed 6.5) which had lost IL-3 dependence on mutagen-induced loss of Pten. Loss of Pten and IL-3 dependence coincided with addiction to the mTOR pathway. Mutant 6.5 was derived from a previously described (Nair *et al*., 1992) v-H-ras-expressing, but IL-3-dependent, parental mast cell line (15V4) by frame-shift mutagenesis with ICR191 and subsequent selection for IL-3-independent outgrowth (Figure 1a). A guanosyl insertion in codon 44 of the Pten gene generated a premature termination codon at position 51 (Figure 1b) in one allele, while the remaining wild-type allele was lost as determined by genomic DNA sequencing (data not shown). Pten protein was undetectable in 6.5 cells compared with parental 15V4 cells (Figure 1c). Lack of Pten activity resulted in constitutive activation of the PI3K-mTORC2-PKB pathway and mTOR addiction as indicated by hyperphosphorylation of protein kinase B (PKB) at position S473 (Figure 1c), an mTORC2 target phosphorylation site, and by hyperphosphorylation of NDRG1 at position T346 (Supplementary Figure 1), an serum/glucocorticoid-regulated kinase 1 (SGK1)-dependent readout for mTORC2 activity (Murray *et al.,* 2004). The mTORC1 downstream targets S6K1-T389 and 4EBP1-S65 were not hyperphosphorylated in mutant 6.5 compared with precursor 15V4 (Figure 1c, Supplementary Figure 1). Nevertheless, these changes correlated with sensitivity of proliferation to long-term rapamycin treatment (Figure 1d, red circles). Inhibition of mTORC2 activity by long-term treatment with rapamycin triggered apoptosis in 42% of cells (Figure 1e). Furthermore, knockdown of the essential mTORC2 component rictor fully inhibited proliferation of 6.5 cells in the absence of IL-3 (Figure 2a, right panel, red circles). Conversely, knockdown of the mTOR complex 1 (mTORC1) component raptor had only a minor effect, in keeping with the observation that the mTORC1 target S6K1 was not hyperphosphorylated in mutant 6.5 (Figure 1c). The knockdown efficiencies of rictor and raptor were comparable (Figure 2b). Raptor knockdown also led to reduced cell volume (Figure 2c) showing that raptor downregulation does have physiological consequences in 6.5 but is not critical for IL-3-independent growth. Knockdown of rictor, similar to rapamycin treatment, triggered substantial apoptosis (55%), with a considerably lesser effect of raptor knockdown (33%) (Figure 2d). These findings indicate that proliferation of mutant 6.5 in the absence of IL-3 is supported by mTOR mainly via mTORC2.

Importantly, and fundamental to our screen, addition of IL-3 suppressed the addiction to mTORC2. Addition of IL-3 countered the inhibition of proliferation (Figure 1d, blue squares) and induction of apoptosis by long-term rapamycin treatment (Figure 1e, right panel, blue line), IL-3 similarly abrogated the inhibitory effect of rictor knockdown in 6.5 cells (Figure 2a, left panel) and suppressed induction of apoptosis following reduction of rictor (Figure 2d, middle panel, blue line). The IL-3-dependent parental cell line 15V4, in contrast, was insensitive to knockdown of rictor or raptor (data not shown). These findings suggest that the Pten mutant 6.5 is sustained by different signalling pathways depending on whether it is growing in the presence or absence of IL-3. With IL-3, growth signals are transmitted via the Jak-Stat pathway as previously shown for the parental cell line (Kiser *et al.,* 2006). In the absence of IL-3, the mTORC2 pathway provides an alternative growth mode that compensates for the absence of Jak-Stat signalling but consequently results in mTOR (mTORC2) pathway addiction. Acquisition of growth factor or cytokine independence is a hallmark of cancer, and mutant 6.5, in contrast to its IL-3-dependent precursor, forms rapidly growing tumors in syngeneic mice (unpublished data). Thus, 6.5 cells offered the possibility, via a genome-wide shRNA screen, to identify genes specifically required for IL-3-independent, mTORC2-addicted proliferation. Identified genes might encode essential driver proteins of oncogenicity and represent potential drug targets.

Identifying genes required for mTORC2-addicted, IL-3-independent proliferation

The overall screening strategy in which we exploited 6.5 cells to identify oncogenicity drivers is shown in Figure 3. We used the TRC lentiviral shRNA library developed by The RNA interference consortium

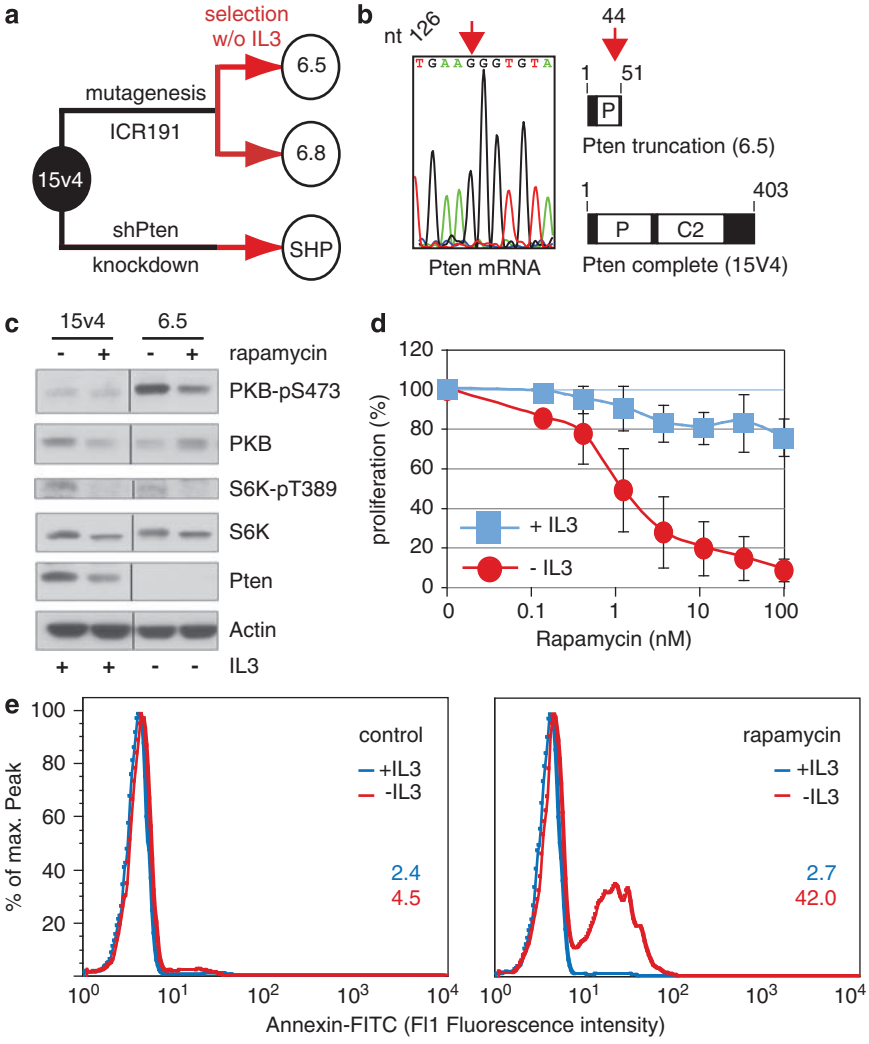

Figure 1 mTOR-addicted Pten mutant 6.5, the target cell of the screen. (**a**) Cell background. From v-H-ras-expressing but still IL-3-dependent parental 15V4 mast cells, IL-3-independent cells were generated following treatment with the frameshift mutagen ICR191 (mutants 6.5 and 6.8) or following stable knockdown of Pten with a shPten-containing lentivirus (SHP line). **b–e** show results obtained with mutant 6.5. (**b**) Loss of Pten. Insertion of a G residue (arrow) at nucleotide position 130 led to a premature termination codon at amino acid position 51. The normal allele was lost and non-detectable by PCR and sequencing. (**c**) Western blots. Pten detection and phosphorylation status of the mTOR targets PKB-pS473 and S6K-pT389 in parental 15V4 and mutant 6.5 with/without rapamycin (20 nM) for 8 h. (**d**) Rapamycin sensitivity. Effect of rapamycin on proliferation in presence (blue squares) or absence (red circles) of IL-3 was measured after 48 h. (**e**) FACS analysis. In all, 6.5 cells were treated for 48 h with rapamycin (50 nM) and apoptotic cells quantified by annexin V staining. Red and blue numbers correspond percentages of apoptotic cells without and with IL-3, respectively. C2, C2 domain; P, phosphatase domain.

(Root *et al.*, 2006). This library targets over 13 000 murine genes, with an average of 5 shRNAs per gene. Using a robotic platform and an arrayed format, 6.5 cells were separately infected with each shRNA virus in individual wells and assayed for proliferation. Cells were infected at a multiplicity of infection ~1, and after allowing 24 h for resistance marker expression, each master plate was split into replica plates containing medium either with or without IL-3, and puromycin to remove non-infected cells. After 5 days, alamarBlue was added to determine the number of viable cells. A non-targeting shControl virus and an shRictor virus were included on each microtiter plate as negative and positive controls, respectively. For each virus, a ratio of inhibition (RI) was calculated by dividing $\text{proliferation}_{+\text{IL3}}/\text{proliferation}_{-\text{IL3}}$ normalized to infection by the non-targeting shControl virus. For example, an RI value of 5 indicates 80% inhibition of normalized proliferation. In a quality control pre-experiment with these control viruses, no false-positive or -negative results were observed (Supplementary Figure 2). Figure 4a shows the values obtained for shControl (blue line) and shRictor (red line) viral infections from a subset of 800 microtiter plates processed during the screen. In the absence of IL-3, knockdown of rictor led to a 10-fold (mean)/23-fold (median) reduction of proliferation compared with the shControl. Thus, the experimental system was sufficiently robust to identify

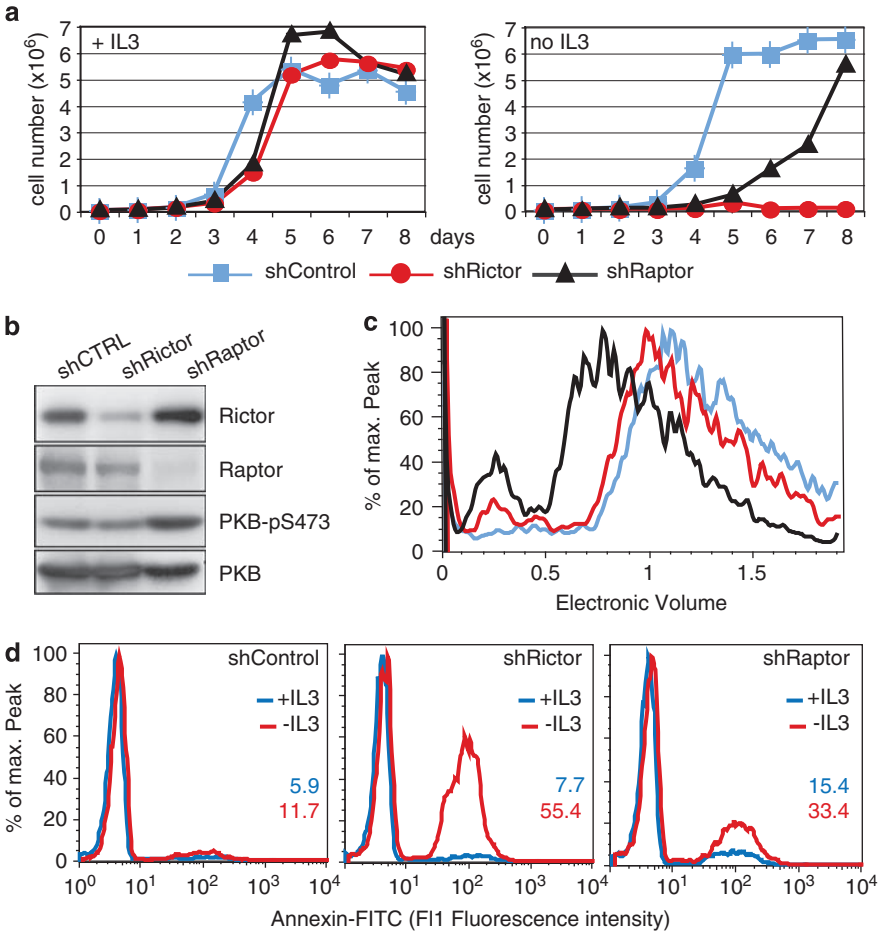

Figure 2 Knockdown of rictor and raptor. (**a**) Requirement of rictor and raptor for IL3-independent growth. Mutant 6.5 cells were infected with shRictor (red circles), shRaptor (black triangles) or shControl virus (blue squares) and after eliminating non-infected cells by puromycin, proliferation was quantified in presence (left panel) and absence of IL-3 (right panel) by cell counting. (**b**) Efficiency of rictor/raptor knockdown determined by western blotting. (**c**) Knockdown of raptor leads to reduction of cell volume. Cells were infected in presence of IL-3 with shControl (blue), shRaptor (black), or shRictor (red) viruses and the cell volume was determined by electronic volume detection using Cell-Lab Quanta (BeckmanCoulter, Brea, CA, USA). (**d**) Induction of apoptosis. Knockdown of rictor leads to substantial apoptosis (middle panel, right peak shown in blue). In presence of IL-3, no apoptosis occurs (red lines). Blue and red numbers indicate percentage of apoptosis in presence and absence, respectively, of IL-3.

shRNAs that inhibited proliferation specifically in the absence of IL-3 (also see Supplementary Figure 3 for further validation of the screen).

A total of 13 408 genes were interrogated in 6.5 cells with 5 or more shRNAs per gene. The relative proliferation for each gene knockdown (versus shControl virus) in the presence (x axis) and absence (y axis) of IL-3 is shown in the scatter plots of Figure 4b (right and left panels). In the left panel (Figure 4b), each point represents the mean for all shRNAs tested per gene (mostly 5), while the right panel shows the mean of the three shRNAs with strongest inhibition of proliferation without IL-3, as calculated by the RI defined above. The points of this second scatter plot (Figure 4b, right panel), as expected because of the removal of data from presumably non-performing constructs, are skewed toward the lower right quadrant. It is noteworthy that no hits appeared in the upper left quadrant, in which one would expect to find genes whose knockdown is inhibitory only in the presence of IL-3. Hits of this nature were not expected because even if IL-3 signalling was blocked through knockdown of a downstream effector, the Pten mutant 6.5 would still have the option of growth via the alternative mTOR mode. The lack of hits in the upper left quadrant indicates that the screen behaved as expected and that the biology of Pten mutant 6.5 was sound.

For follow-up analysis, we selected the top 800 genes from the above screen. These genes correspond to the shRNAs that selectively inhibited mTOR-addicted growth with an RI > 7.3 and are hereafter designated group 'A' genes (shaded area in Figure 4b, right panel). Group A genes are listed in Supplementary Table 1. Gratifyingly, this group includes the genes for mTOR (RI 14.2) and phospholipase D1 (RI 17.6). The mTORC2 component rictor was positive with only two oligos in the screen, and was therefore below the cutoff value. In follow-up experiments, however, these two oligos were nevertheless included in the screen, they were consistently and strongly positive (see below). We

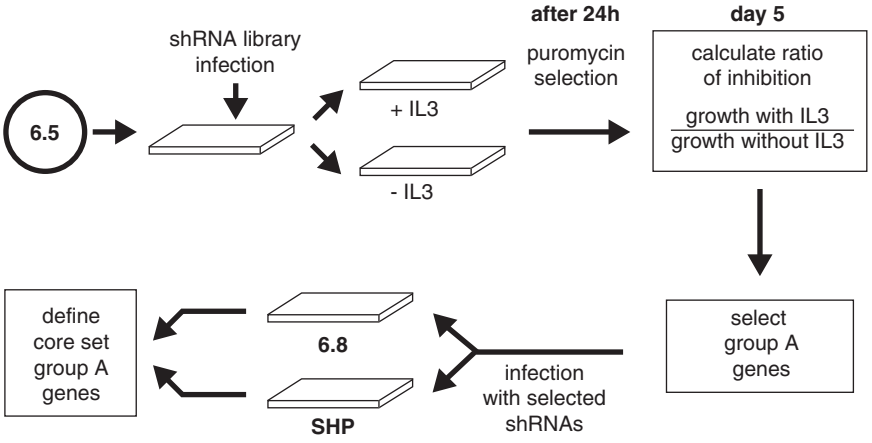

Figure 3 Flow scheme of screening procedure. 6.5 cells (3000) were infected with single lentiviruses (multiplicity of infection (m.o.i.) of 1) carrying shRNA targeting sequences and a puromycin-resistance gene in individual wells using a robotic platform. After 24 h, plates were split in parallel plates with/without IL-3 and containing puromycin to remove non-infected cells. On day 5, relative growth (compared to infection with shControl virus) was quantified by measuring cell proliferation with AlamarBlue, and a RI was calculated proliferation + IL-3/proliferation–IL-3. For further analysis, hits with a ratio >7.3 (calculated using the three oligos with the highest RI, and eliminating genes in which only one oligo was positive) were confirmed by re-infection of lines 6.8 and SHP with two lentiviruses per gene using the two oligos with the highest RI. This allowed definition of a core set of group A genes with RI >7.3 and being essential in 6.5, 6.8 and SHP cells.

note that, for technical reasons, shRNAs targeting the mTORC2 component mSIN1 were not included in the screen. Phospholipase D1 (Pld1) generates phosphatidic acid, which has been shown to activate mTOR in many contexts (Foster, 2007). The Pld1 inhibitor 1-butanol, but not its non-inhibitory structural analogue tert-butanol, strongly inhibited IL-3-independent proliferation of mutant 6.5, and also decreased PKB and S6K phosphorylation (Figures 5a and b). For comparison, we also selected the top 800 genes whose knockdown inhibited proliferation of 6.5 cells both in the presence and absence of IL-3. In each case, the inhibition of proliferation relative to a control virus was >80%. This second group of genes was designated group 'B' and is graphically represented as the points to the left of the vertical line in Figure 4b. Group B genes are listed in Supplementary Table 2. Thus, group A contains genes whose knockdown is conditionally toxic (only in the absence of IL-3) whereas group B contains genes whose knockdown is generally toxic.

Positive gene enrichment analysis for group A and B genes

To test whether our screen had enriched for genes linked to specific biological processes, we performed gene set enrichment analysis with the 800 group A and 800 group B genes, and with an equal number of randomly selected genes, using commercial software (Ingenuity Systems, www.ingenuity.com). We observed for both group A and B a highly significant enrichment of genes associated with several functional categories and canonical pathways (Figure 4c, group A hits shown on the left in blue, group B on the right in red, randomly selected control genes in grey). Group A contained genes associated with hematological disease, signalling, cancer and mitochondrial dysfunction. Group B was enriched in functions such as protein synthesis, cell cycle and Huntington disease signalling. Both group A and B were enriched in genes related to cell death. In contrast, the 800 randomly selected genes displayed no evidence of specific enrichment (grey bars in Figure 4c). Thus, as expected, the group A and B genes are qualitatively different.

To uncover other qualitative differences between the genes of groups A and B, we compared these hits with genes that are generally essential in many different cancer lines (Luo *et al.,* 2008). With a sub-library of the human counterpart of the TRC library used here, Luo *et al*. (2008) recently identified a set of 268 genes whose knockdown inhibited proliferation in at least 8 out of 12 human cancer lines tested. Comparing this set of genes with our A and B genes, we noted a strong overlap of 52 genes with group B (P-value = 6.24E-38; q-value = 8.58E-34), including a strong representation of ribosomal protein genes (Supplementary Table 3). Interestingly, an overlap of only 7 genes was detected with the 800 genes of group A (listed in Supplementary Table 3, at bottom). The observation that only group B is enriched in genes commonly required in a broad panel of cancer cell lines again suggests that group A and B genes differ qualitatively. Furthermore, the finding that group A genes were rarely detected in a screen based on general toxicity in conventional cancer cell lines suggests that our novel conditional screen might identify new oncogenicity genes.

We analyzed whether groups A and B include genes encoding known targets of anticancer drugs, in particular signalling inhibitors (Ingenuity Systems software). Group A contained genes for nine drug targets, namely mTOR (rapamycin; kidney cancer), the membrane protein CD52 (alemtuzumab; chronic lymphocytic leukemia), the farnesyltransferase Fnta (lonafarnib; solid tumors), the signalling kinase MAPK14 (known as p38) (RO-3201195; early clinical trials), the membrane protein

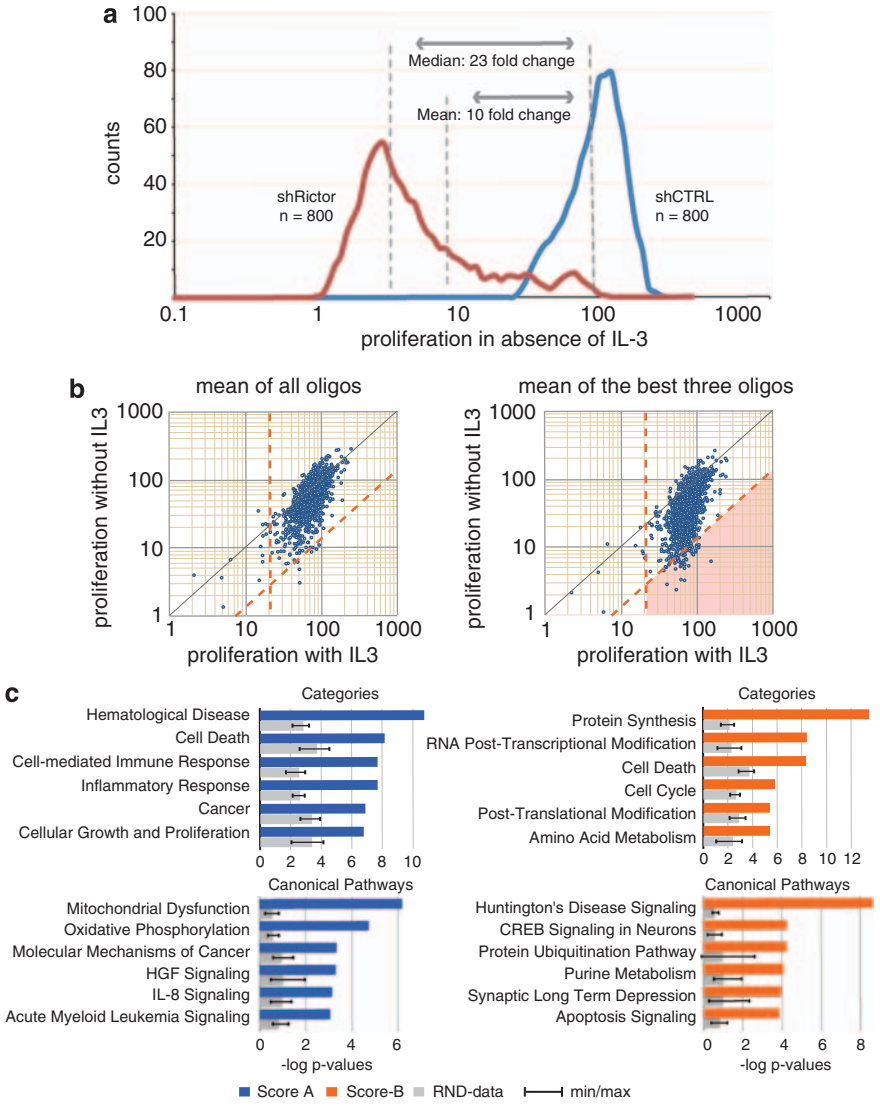

Figure 4 Screening results: group A and B hits. (**a**) Quality control and reference values. Each microtiter plate contained one well infected with shControl (blue) and shRictor (red) viruses, for negative and positive control, respectively. Proliferation in absence of IL-3 is shown. Mean and median values are shown, with both values coinciding for the shControl virus. Values are taken from 800 plates. (**b**) Scatter plots. Relative growth with IL-3 (*x* axis) plotted against relative growth without IL-3 (*y* axis). In the left panel, each dot represents the mean value of all oligos per gene (usually five). In the right panel, the three oligos with the highest RI (proliferation + IL-3/proliferation–IL-3) were used to calculate the mean. Values within the shaded area have a RI >7.3, (corresponding to $>84\%$ growth inhibition in absence of IL-3) and constitute the gene A set. Values to the left of the dotted vertical line ($<20\%$ proliferation with IL-3) constitute the gene B set. (**c**) Gene enrichment analysis. Using Ingenuity software, statistically significant enrichment of categories and pathways for the 800 group A genes (left, blue bars) and the 800 group B genes (right, red bars) are shown. In all, 800 randomly selected genes served as a control set (grey bars).

MS4A1/CD20 (rituximab; non-Hodgkin lymphomas), the platelet derived growth factor (PDGF) receptors A and B (sunitinib, kidney cancer), the protein kinase C isoform PKCCB (enzastaurin; glioblastoma), the signalling kinase Raf1 (sorafenib; kidney and other cancers) and the vascular endothelial growth factor VEGFA (bevacizumab; colon and other cancers). Group B revealed only one known cancer drug target, the growth factor receptor protein FGFR1 (pazopanib; angiogenesis inhibitor). Thus, group A is enriched in genes for known and presumably new potential targets of pharmacological signalling inhibitors.

mTORC2-addicted growth relies on mitochondrial function

As shown in Figure 4c, group B is highly significantly enriched for functions related to protein synthesis. This nicely illustrates the discriminating power of the screening system, as basic functions such as translation would be required regardless of IL-3 signalling and mTOR addiction. An unexpected observation, however, was that group B contained genes for 51/78 cytoplasmic ribosomal proteins, but only one mitochondrial ribosomal protein. Conversely, group A contained genes for 10/53 mitochondrial ribosomal proteins, and none

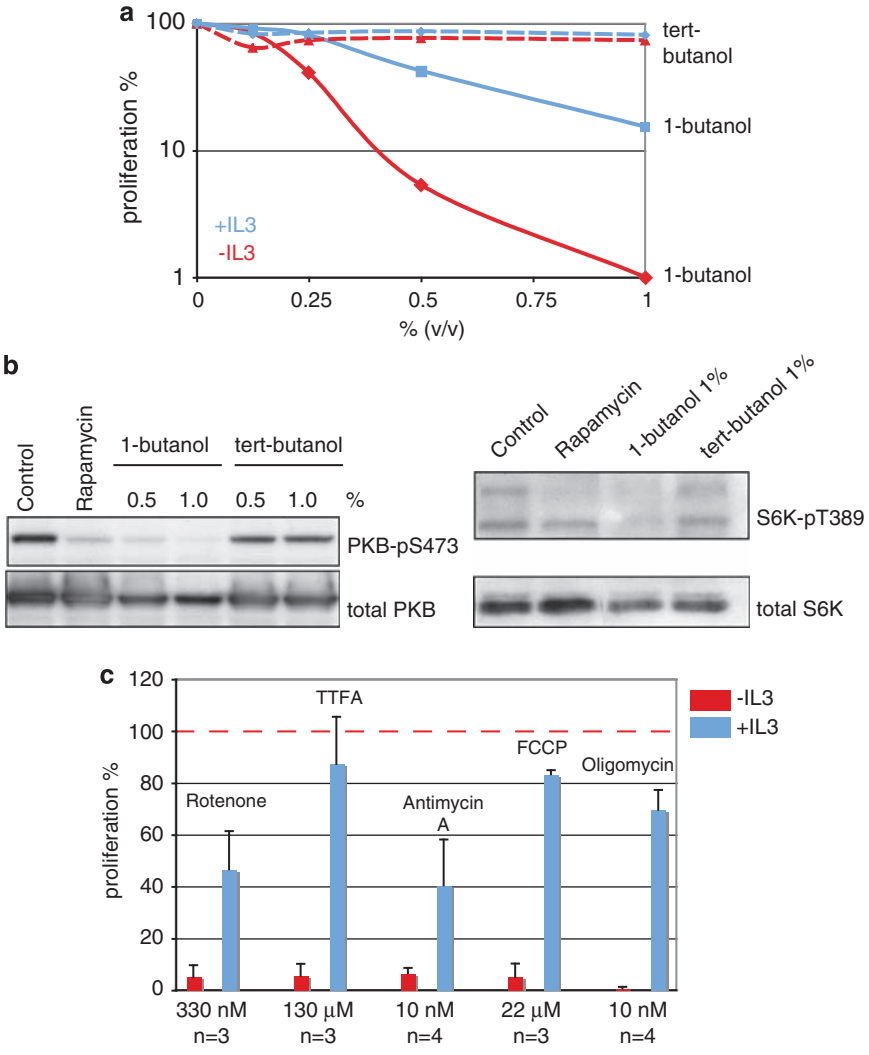

Figure 5 Sensitivity of mutant 6.5 in absence of IL-3 to specific inhibitors. (**a**) Requirement for phospholipase D1. In all, 6.5 cells were incubated with increasing amounts of the Pld1 inhibitor 1-butanol (solid lines) or the inert tert-butanol (broken lines) in presence (blue squares) and absence (red diamonds) of IL-3 and proliferation was measured after 48 h by alamarBlue staining. (**b**) Effect of 1-butanol. Cells were incubated with the indicated reagents for 6 h and total protein lysate was processed for western blots. (**c**) Effect of mitochondrial inhibition. Cells were incubated with the indicated respiratory chain inhibitors in presence (blue) and absence (red) of IL-3. Concentrations used and number of experiments to calculate the mean are indicated. Results were normalized to untreated controls in presence or absence of IL-3 (dashed red line).

Table 1 Requirement for cytoplasmic and mitochondrial ribosomal protein genes

	Mitochondrial ribosomal proteins	*Cytoplasmic ribosomal proteins (L-subunit)*	*Cytoplasmic ribosomal proteins (S-subunit)*
Group A genes	10/53[a]	0/43	0/35
Group B genes	1/53[b]	30/43[c]	21/35[d]

[a]Mrpl9, Mrpl10, Mrpl13, Mrpl15, Mrpl27, Mrpl49, Mrpl5, Mrps2, Mrps18b, Mrps33.
[b]Mrpl34.
[c]Rpl3, Rpl4, Rpl6, Rpl8, Rpl9, Rpl10a, Rpl11, Rpl12, Rpl13, Rpl13a, Rpl14, Rpl15, Rpl17, Rpl18, Rpl18a, Rpl19, Rpl23, Rpl23a, Rpl24, Rpl26, Rpl30, Rpl31, Rpl32, Rpl35, Rpl35a, Rpl36, Rpl37, Rpl37a, Rpl38, Rpl39.
[d]Rps2, Rps3, Rps3a, Rps4x, Rps5, Rps7, Rps8, Rps10, Rps11, Rps13, Rps14, Rps16, Rps17, Rps19, Rps20, Rps24, Rps26, Rps27a, Rps28, Rps29, Rpsa.

for cytoplasmic ribosomal proteins (0/78; Table 1). These findings suggest that 6.5 cells growing in the mTOR-addicted mode rely heavily on mitochondrial function but this can be dispensed with if a growth input from IL-3 is supplied. To investigate this notion further, we examined the 800 group A genes for additional mitochondrial functions, in particular genes related to the respiratory chain and adenosine triphosphate (ATP)

Table 2 Respiratory chain and mitochondrial ATP synthase genes

	Complex I	*Complex II*	*Complex III*	*Complex IV*[a]	*ATP synthase*
Group A genes[b]	6/34	1/4	3/9	9/22	5/16
Group B genes[c]	1/34	0/4	0/9	0/22	1/16

Abbreviation: ATP, adenosine triphosphate.
None of the mitochondrial-encoded components were targeted by the library.
[a]Complex IV isoforms were included.
[b]Complex I: Ndufa3, Ndufa5, Ndufa12, Ndufaf4, Ndufb3, Ndufb10. Complex II: Sdhb. Complex III: Uqcrh, Uqcrfs1, Uqcrb. Complex IV: Cox5a, Cox5b, Cox6a1, Cox6a2, Cox6b1, Cox6c, Cox7b, Cox7a2l, Cox8b. ATP Synthase: ATP5d, ATP5 h, ATP5k, ATP5 l, ATP50.
[c]Complex I: NdufbV. Complex V: ATP5e.

synthesis. Group A contained many hits in components of respiratory chain complexes I, II, III and IV (Cox 5a, Cox5b, Cox6a1, Cox6a2, Cox6b1, Cox6c, Cox7a2l, Cox7b, Cox8b, Ndufa3, Ndufa12, Ndufb10, Sdhb, Uqcrb, Uqcrfs1 and Uqcrh), and ATP synthase (Atp5d, Atp5 h and Atp5k), and two ATP synthase assembly factors (Atpaf1 and Atpaf2) (Table 2). Also included was the mitochondrial fission factor 5230400G24Rik (Gandre-Babbe and van der Bliek, 2008), a gene driving mitochondrial replication.

To confirm if mitochondrial activity is indeed more critical for 6.5 cells when growing in the absence of IL-3, we challenged 6.5 cells with inhibitors of the respiratory chain, including rotenone, thenoyltrifluoroacetone, antimycin A, FCCP (carbonyl cyanide 4-(trifluoromethoxy) phenylhydrazone) and oligomycin. As shown in Figure 5c, mutant 6.5 is markedly more sensitive to perturbation of mitochondrial activity when grown in the absence of IL-3. These inhibitors caused apoptosis in 6.5 cells, again only in absence of IL-3 (Supplementary Figure 4). Thus, the transformed growth mode (IL-3 independent/mTORC2 addiction), but not the normal growth mode, of 6.5 cells relies heavily on mitochondrial activity.

mTORC2 addiction and glucose metabolism

Transformed cells have a greatly increased demand for glucose as they inefficiently generate ATP via aerobic glycolysis, the so-called Warburg effect. Group A contained a significant number of genes related to glucose metabolism (Supplementary Figure 5, group A hits are indicated in red, for RI values see Supplementary Table 1), including Glut1, Glut4, Hk2, Gpi1 and Pgls, while Pfk1, Pfk2 and G6pdx were slightly below the cut-off RI of group A genes. Glut1 and Glut4 are glucose transporters. Glut4 is normally present on intracellular vesicles but translocates to the plasma membrane on insulin stimulation via PKB signalling (Hill *et al.,* 1999; Wang *et al.,* 1999) which is constitutively high in mutant 6.5. Significantly, PKB and other factors reported to be essential in Glut4 translocation, namely PKCz and Pld1 (Bandyopadhyay *et al.,* 2001; Heyward *et al.,* 2008) were also represented in group A. Hk2 and Gpi1 catalyze the two first steps in the glycolytic pathway. Pfk1 catalyzes the rate-limiting step that irreversibly commits glucose to the glycolytic pathway. Pfk1 is allosterically inhibited by ATP but this is overcome through allosteric activation by fructose-2,6-bisphosphate. Fructose-2,6-bisphosphate is produced from fructose-6-phosphate through a side reaction by Pfk2. G6pdx catalyzes the first and rate-limiting step in the pentose phosphate pathway. Pgls catalyzes the second step in the pentose phosphate pathway. Collectively, these data suggest that mTORC2-addicted Pten-deficient cells have a high demand for glucose typical of transformed cells.

Defining a core set of 47 genes linked to mTORC2 addiction

We wished to restrict our list of group A genes to genes that are also essential in other Pten-deficient cell lines, thus defining a core set of essential group A genes. For this analysis, we selected 235 group A genes with particularly high RI scores and used the two most effective, corresponding shRNAs for knockdown in two isogenic Pten-deficient cell lines 6.8 and SHP. Cell line 6.8 was derived by mutagenesis from the same parental cell that produced 6.5 (Figure 1a) but contains a different Pten frameshift mutation (Supplementary Figure 6). SHP was generated by stably knocking down Pten by lentiviral shRNA infection in the same parental 15V4 cell line as 6.5 and 6.8, and shares many of their properties, including rapamycin sensitivity and rescue by IL-3, as shown in Supplementary Figure 7. In all, 47 out of the selected 235 group A genes were essential in 6.5, 6.8 and SHP cells grown in the absence of IL-3 (Table 3). Approximately half of the 235 group A genes were essential in any two of the three cell lines tested. Thus, we defined a core set of 47 genes that are critically required for growth specifically in mTORC2-addicted cells (Table 3). We note that the genes for mTOR and the mTORC2 component rictor (4921505C17Rik) are part of this core set. Consistent with our above observation that mTORC2 addiction requires mitochondrial activity, the core set of genes also contained genes encoding mitochondria-related functions, in particular the mitochondrial ribosomal protein Mrpl27, the respiratory chain proteins Cox7a21 and Uqcrb, and seven additional proteins with reported mitochondrial localization or association. The seven additional proteins were Rab32 (Alto *et al.,* 2002), the prolyl hydroxylase Egln3/Phd3 (Lipscomb *et al.,* 2001), the differentiation associated protein Mmd2 (Gonez

Table 3 Forty-seven genes from group A required also in 6.8 and SHP cells

Gene symbol	*Gene description*	*RI (mean of two oligos) 6.8*[a]	*RI (mean of two oligos) SHP*[a]
1110028C15Rik	RIKEN cDNA 1110028C15 gene	5.4	5.9
2900006B13Rik	RIKEN cDNA 2900006B13 gene	13.3	9.6
4921505C17Rik	Rictor	76.4	10.3
5230400G24Rik	RIKEN cDNA 5230400G24 gene	32.1	6.4
Abca3	ATP-binding cassette	33.3	30.4
Alox15	Arachidonate 15-lipoxygenase	43.9	8.4
Aqp1	Aquaporin 1	30.7	6.4
Aqp7	Aquaporin 7	64.7	23.1
Arsb	Arylsulfatase B	19.4	26.8
Asb15	Ankyrin repeat and SOCS box-containing protein 15	65.6	8.5
Atp1b3	ATPase	33.3	15.2
Atp6v0c	ATPase	15.6	13.8
Cbx2	Chromobox homolog 2 (Drosophila Pc class)	8	7.2
Clps	Colipase	66.4	5.1
Cnga4	Cyclic nucleotide-gated channel α 4	43.2	23.6
Cox7a2l	Cytochrome c oxidase subunit VIIa polypeptide 2-like	12.9	26.9
Cpa3	Carboxypeptidase A3	15.2	5.2
Csh2	Chorionic somatomammotropin hormone 2	8.6	12.1
D11Ertd333e	DNA segment	54.9	5.4
Deadc1	Deaminase domain-containing 1	19.3	9
Dmgdh	Dimethylglycine dehydrogenase precursor	23.5	17.3
Egln3	EGL nine homolog 3 (C. elegans)	14.9	9.2
Eml4	Echinoderm microtubule-associated protein- like 4	67.2	20.6
Fhl3	Four and a half LIM domains 3	63.6	34.6
Frap1 (mTOR)	FK506-binding protein 12-rapamycin-associated protein 1	69.7	64.9
Gab1	Growth factor receptor-bound protein 2-associated protein 1	12.7	9.9
H2-Ab1	Histocompatibility 2	45	20.4
Il1f5	Interleukin 1 family	86.7	16.1
Kctd11	Potassium channel tetramerization domain-containing 11	29.4	5.4
LOC279880	Similar to aspartate aminotransferase	29.7	11.4
LOC546723	Similar to protein phosphatase 1	19.2	5.4
Mmd2	Monocyte to macrophage differentiation-associated 2	16.6	13.2
Mrpl27	Mitochondrial ribosomal protein L27	24.8	28.3
Ms4a1	Membrane-spanning 4-domains	44.6	15.9
Nalp4f	NACHT	51.7	11.3
Pira4	Paired-Ig-like receptor A4	84.6	13.5
Plxna4	Plexin A4	19	5.1
Ppp1r1a	Protein phosphatase 1	24.7	6
Prdm4	PR domain-containing 4	89	55.7
Rab32	RAB32	48	13.1
Rab33a	RAB33A	46.2	26.8
Rpa2	Replication protein A2	13.8	5.2
S100a11	S100 calcium-binding protein A11 (calizzarin)	11.3	24.9
Sfn	Stratifin	30.4	23.6
Sh3bp2	SH3 domain-binding protein 2	40.8	5.8
Tmc6	Transmembrane channel-like gene family 6	24.1	8.6
Uqcrb	Ubiquinol-cytochrome c reductase-binding protein	29.4	18

Abbreviations: ATP, adenosine triphosphate; cDNA, complementary DNA, RI, ratio of inhibition.
[a]RI indicates relative proliferation in presence of IL-3 divided by relative proliferation in absence of IL-3.

et al., 2008), D11ertd333e/Slc25a39 (Nilsson *et al.,* 2009), 2900006B13Rik/Agxt2l2, (Pagliarini *et al.,* 2008), dimethylglycine dehydrogenase Dmgdh (Wittwer and Wagner, 1980) and mitochondrial fission factor/5230400G24Rik (Gandre-Babbe and van der Bliek, 2008).

Analysis of mTORC2 addiction genes in human cancer cell lines

We wished to determine whether genes required on mTORC2 addiction in mouse cells are also essential in human cancer cells. Small interfering RNAs (siRNAs) against human orthologs of 24 of the 47 core group A genes (listed in Supplementary Table 4) were tested in the human cancer cell lines A549 (carcinomic human type II alveolar epithelial cells) and H1299 (non-small cell carcinoma of lung), and in two human normal fibroblast lines. A549 cells were chosen as an example of tumor cells with K-ras activation (www.sanger.ac.uk), whereas H1299 cells lack Pten because of methylation of the Pten promoter (Soria *et al.,* 2002). In each case, we used pools of four siRNA oligos per gene (Dharmacon SMARTpool). Negative and positive controls were a non-targeting siRNA (siNON) and a cytotoxic siRNA (siDeath), respectively, shown on the left in the panels of

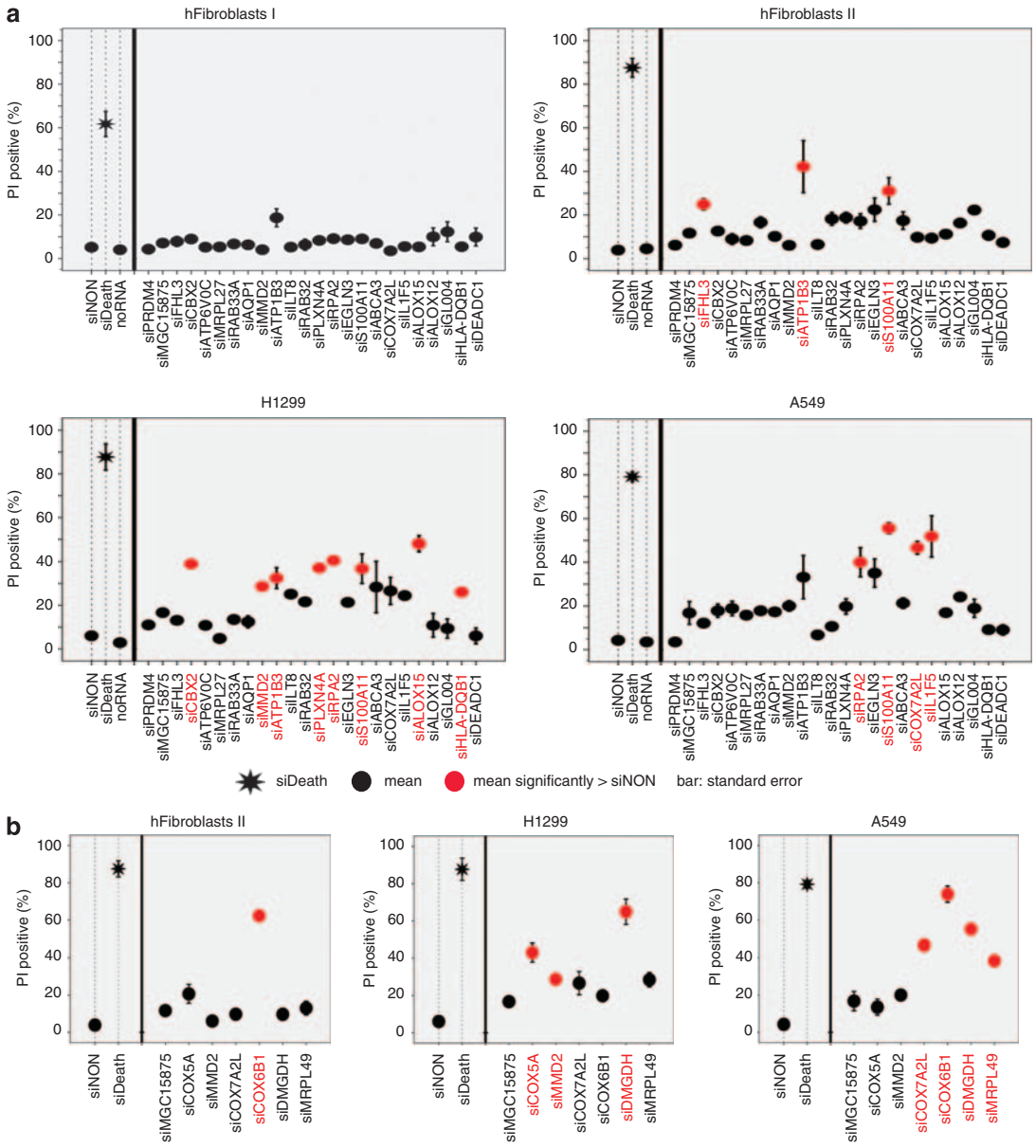

Figure 6 Induction of cell death in human cancer lines. (**a**) Analysis of 24 human orthologs of the core set of 47 genes. Two human cancer lines (H1299, A549) and two human normal fibroblast lines (I, II) transfected with SMARTpool siRNA pools of four oligos (Dharmacon), with non-targeting siNON and cytotoxic siDeath as respective negative and positive controls. PI-positive cells were measured after 96 h. Shown are the mean percentage of PI-positive cells from two or three replicate experiments with standard errors. For analysis of significance, genes were normalized to siDeath (100%) and siNON (0%). Genes were scored positive (shown in red) for cell death if the normalized mean for PI-positive cells exceeded 25% and the distance between twice the standard errors of siNON and target was larger than 15%. Controls (siNon, siDeath, noRNA) are shown to the left in each panel. (**b**) Analysis of seven mitochondrial genes was performed as in **a**.

Figure 6. At 96 h after transfection, cell viability was quantified by propidium iodide (PI) staining. Figure 6a shows the results from two or three replicate experiments, in which genes scoring statistically positive (see legend of Figure 6) are shown in red. Of the 24 genes examined, three were essential in one of the two normal fibroblast lines tested (FHL3, ATP1B3, S100A11). Excluding these three essential genes, eight genes were essential in at least one cancer cell line, with Rpa2 encoding a replication protein being essential in both lines tested. Thus, a significant fraction of genes identified via the IL-3-based screen in murine cells are also essential for proliferation in human cancer cell lines, and the corresponding proteins can be considered potential therapeutic targets.

We also targeted seven group A genes encoding mitochondrial proteins (Supplementary Table 4) in the above human cancer cell lines. We found that knockdown of six of these genes conferred significant toxicity in at least one tumor cell line, while knockdown of only one

(COX6B1) was toxic in normal fibroblasts (Figure 6b, red symbols). Thus, mitochondrial function also appears to be particularly important in at least some human cancer cells, as in murine Pten-deficient, mTOR-addicted cells.

Discussion

Acquisition of growth factor independence and signalling pathway addiction are important steps in oncogenesis. We have identified, by a genome-wide shRNA screen, a group of genes (group A genes) whose knockdown is selectively lethal in growth factor (IL-3) independent, mTOR pathway (mainly mTORC2) addicted cells. Importantly, we found that a significant fraction of these genes are also essential in human cancer cells but not in normal fibroblasts. Thus, group A genes may encode novel anticancer drug targets.

A major observation was that many of the genes (group A) required on mTOR addiction encode mitochondrial functions. These mitochondrial functions included components of respiratory chain complexes I through IV, components of the ATP synthase complex, nuclear-encoded components of mitochondrial ribosomes and the transcription factor YY1. Also included was the mitochondrial fission factor (Mff/5230400G24Rik) that controls mitochondrial division (Gandre-Babbe and van der Bliek, 2008) and was, notably found in the core set of 47 group A genes. These data suggest that mTOR signalling is linked to mitochondrial function. Indeed, links between mTOR, particularly mTORC1 and mitochondria have been reported previously (Schieke *et al.,* 2006; Cunningham *et al.,* 2007; Bentzinger *et al.,* 2008; Polak *et al.,* 2008; Ramanathan and Schreiber, 2009). Furthermore, Cunningham *et al*. (2007) showed that mTOR forms a complex with the transcription factors YY1 and PGC1. YY1 and PGC1 mediate expression of nuclear genes encoding mitochondrial functions. YY1 is a group A hit with an RI value 10.4. As there are many ways by which mitochondrial function can be pharmacologically perturbed, it may represent an Achilles' heel in mTOR-addicted cells.

Why are mTORC2-addicted cells dependent on mitochondria? In other words, what do mitochondria provide that is essential in mTORC2-addicted cells? There are several nonexclusive possibilities including ATP synthesis, reactive oxygen species (ROS) production and inhibition of apoptosis. A requirement for mitochondria in the production of ATP is directly supported by group A hits such as those affecting ATP synthase (also see below). Cellular ROS is required for cell proliferation in certain contexts, although excessive ROS levels are toxic (Weinberg *et al.,* 2010). Group A hits include several components from complexes of the respiratory chain, which in addition to their role in ATP production also produce ROS. Consistent with a requirement for ROS, we have observed that our mTORC2-addicted cells indeed have higher levels of ROS compared with non-addicted parental cells (data not shown). Finally, mitochondria have an important role in apoptosis. Metabolically active mitochondria could prevent apoptosis. Accordingly, group A hits that compromise mitochondria function could result in enhanced apoptosis. Consistent with this notion, we observed that inhibition of mTORC2 in our mTOR-addicted cells strongly enhances apoptosis (Figure 1e), and that many group A hits cause enhanced cell death as seen microscopically (data not shown).

Cancer cells are often characterized by increased glucose uptake and aerobic glycolysis, also known as the Warburg effect. This aerobic glycolysis is important for ATP generation but also, together with the pentose phosphate pathway, for generation of redox potential and nucleic acid and fatty acid precursors. A number of group A genes were related to glucose transport (Glut1, Glut4) and initial steps of the glycolytic pathway (Hk2, Gpi and Pfk1). This suggests that our mTOR-addicted cells are dependent on the so-called Warburg effect. However, phosphoglycerate kinase (Pgk1, Pgk2) and pyruvate kinase (Pklr), two downstream enzymes that catalyze the ATP-generating steps of glycolysis, were not group A hits. This suggests that mTOR-addicted cells generate ATP via mitochondrial oxidative phosphorylation, consistent with our above observation that mitochondrial ATP synthesis is important. Although aerobic glycolysis is important for the transformed state, this does not preclude a role for mitochondria in ATP generation. Weinberg and Chandel (2009) have shown that tumors generate ATP via both glycolysis and oxidative phosphorylation. Thus, the Warburg effect does not necessarily rule out mitochondrial dependence. Furthermore, there is growing awareness that tumor cells also need mitochondria for reasons other than ATP generation, such as pyrimidine synthesis, fatty acid synthesis and glutaminolysis (Wise *et al*, 2008; Dang, 2010).

Others have reported in a Pten-deficient tumor model upregulation of glycolytic enzymes via mTORC1-dependent stimulation of hypoxia inducible factor 1 (HIF-1) (Majumder *et al.,* 2004). This clearly differs from our mTORC2-dependent system, in which HIF-1a is not upregulated (Supplementary Figure 1, right panel) and knockdown of HIF-1a had no effect on proliferation. Rather, in our mTORC2-dependent system the upregulation of glycolytic enzymes may depend on c-myc. C-myc, its dimerization partner max (Grandori *et al*. 1996) and the myc stimulator mycbp (Jung and Kim, 2005) are all group A genes with RI values of 13.4, 8.7 and 13.4, respectively. Interestingly, c-myc-transformed cells are sensitive to mitochondrial inhibition (Fan *et al*., 2010). Among its many functions, myc stimulates mitochondrial biogenesis, oxygen consumption and glycolysis, suggesting that it drives both aerobic glycolysis and oxidative phosphorylation (Dang, 2010). These findings further indicate that glycolysis and mitochondria are important in transformed and mTORC2-addicted cells.

Why are cells less dependent on mitochondria when grown in the presence of IL-3, as we have observed? IL-3 increases glucose uptake and glycolysis such that energy production by glycolysis exceeds cellular needs (Bauer *et al.,* 2004) which could explain the loss of

mitochondrial dependence when cells proliferate in the presence of IL-3.

Finally, we also investigated whether the human counterparts of group A genes defined in our murine mTOR-addicted cells are also essential in human cancer cells. siRNA against 8 out of 24 group A genes tested inhibited at least one of two human lung cancer cell lines, with no toxicity in normal human fibroblasts. These genes included several mitochondria-related genes (Figure 6). *A priori*, mitochondrial functions would seem unlikely targets for cancer therapy although this has been proposed (Fantin and Leder, 2006). Targeting mitochondria might, however, be an effective therapy against subtypes of tumors displaying enhanced mitochondrial dependence as observed in our mTOR-addicted cells.

Group A contains a sub-set of genes encoding established targets of anticancer drugs. This subset of genes includes oncogenes and non-oncogenes. Prime examples are the mTOR non-oncogene targeted by rapalogs and the Raf1 oncogene targeted by sorafenib. This, and the fact that knockdown of group A genes is selectively (and not generally) toxic, suggests that additional genes from group A may similarly encode therapeutic targets for human cancer. Careful evaluation of group A genes may provide novel leads for drug development. Encouragement in this direction comes from the observation that a substantial fraction of group A genes, for example, 14 out of the core set of 47 A genes (Table 3), encode enzymes in which the design of specific small molecule inhibitors may be feasible. These small inhibitors may target products of heretofore unknown non-oncogenes.

Materials and methods

Cell culture and cell lines

Murine, IL-3-dependent PB-3c mast cells and its derivatives were cultured as described (Kiser *et al.,* 2006). Clone 15 is a subclone of PB-3c; 15V4 is a v-H-ras-expressing clone 15 (Nair *et al.,* 1992). In all, 6.5 and 6.8 are IL-3-independent clones that were isolated from 15V4-GFP after frameshift mutagenesis with ICR191 as described and selected for proliferation in absence of IL-3 (Kiser *et al.,* 2006). IL-3-independent SHP cells were generated from IL-3-dependent 15V4 cells following knockdown of Pten via lentiviral shRNA targeting and simultaneous introduction of the blasticidin-resistance marker. Two normal human fibroblast lines with normal karyotypes derived from skin biopsies were obtained from Dr F Wenzel, University Childrens Hospital, Basel, Switzerland, and maintained in Eagle's minimal essential medium with 10% fetal calf serum, penicillin and streptomycin. H1299 and A549 are human lung cancer lines that were cultured in RPMI 1640 with 10% fetal calf serum, penicillin and streptomycin.

Chemicals and antibodies

Cell culture reagents, puromycin, rapamycin, 1-butanol, tert-butanol and mitochondrial electron transport chain inhibitors: rotenone, oligomycin, antimycin A, TTFA (2-thenoyltrifluoroacetone) and FCCP were obtained from Sigma-Aldrich (St Louis, MO, USA), horseradish peroxidase-coupled anti-mouse and anti-rabbit secondary antibodies were from Pierce (Rockford, IL, USA). Anti-PKB-pS473, anti-S6K-pT389, anti-NDRG1-pT346, anti-S6K1, anti-Pten, anti-Rictor, anti-PKB and anti-Raptor were from Cell Signaling Technology (Beverly, MA, USA), anti-actin from Chemicon (Temecula, CA, USA), anti-NDRG1 (Santa Cruz, Santa Cruz, CA, USA), anti-HIF1a (Bethyl Laboratories, Montgomery, TX, USA) and anti-GAPDH (Abcam, Cambridgeshire, UK).

Selection for IL-3-independent proliferation by viral infection

To assess the effect of selected shRNAs on cellular proliferation, lentiviral particles carrying specific targeting shRNAs and a puromycin-resistance marker were used for infection. Particles were obtained from Sigma-Aldrich at a titer of $1–3 \times 10^7$ transfection units per ml. In all, 5×10^5 15V4 or 6.5 cells were infected in IL-3-containing medium with 5×10^5 transfection units of lentiviral supernatant in presence of 10 μg/ml polybrene. After 12 h, non-infected cells were removed by the addition of puromycin (2 μg/ml) for at least 36 h. After selection, cells were carried without puromycin. To assess for IL-3-independent proliferation, IL-3 was removed by washing twice before 5×10^5 cells were seeded in 10 ml culture medium. Viable cells counts were obtained by PI staining and fluorescence-activated cell sorting (FACS) analysis.

For shRNA-mediated knockdown, the target sequences were 5′-CAACAAGATGAAGAGCACCAA-3′ for a non-targeting control (shControl); 5′-CGACTTAGACTTGACCT ATAT-3′ targeting murine Pten; 5′-CGGTTCATACAAGAG TTATTT-3′ targeting murine Rictor and 5′-GCCCGAG TCTGTGAATGTAAT-3′ targeting murine Raptor.

To generate puromycin-sensitive IL-3-independent SHP cells, we first prepared lentiviral supernatant with the Virapower Bsd expression system (Invitrogen, Carlsbad, CA, USA) following the manufacturer's guidelines and using a shRNA expression cassette from pTER (van de Wetering *et al.,* 2003) that was subcloned into the *Eco*R1 site of a pLenti6/UbC/V5-GW/lacZ vector (Invitrogen), in which the UbC promoter was deleted by digestion with *Bmg*B1 and *Bam*H1. 15V4 cells were infected with Virapower Bsd supernatant for shRNA expression targeting Pten or non-targeting as negative control. At 24-h post-infection, cells were selected with 50 μg/ml blasticidin for at least 72 h and then selected for IL-3 independence. After IL-3 removal, blasticidin resistant cells grew out only on Pten knockdown, but not on expression of non-targeting shRNA.

Western blotting

For cell lysis, cells were washed with phosphate-buffered saline before lysis in ice-cold TNE buffer (50 mM Tris–HCl pH8.0, 150 mM NaCl, 0.5 mM EDTA, 1% Triton X-100 supplemented with protease inhibitors and phosphatase inhibitors (1 × Roche complete protease inhibitor cocktail, 1 μg/ml Aprotinin, 1 μg/ml Pefabloc, 1 mM phenylmethylsulfonyl fluoride, 10 mM NaF, 10 mM NaN_3, 10 mM NaPPi, 10 mM b-glycerophosphate, 10 mM p-nitrophenylphosphate). After 10 min of incubation, cell debris was removed by centrifugation for 15 min at 12 000 *g*. The protein concentration was determined with a Bradford assay (Bio-Rad, Hercules, CA, USA) and equalized among samples. For western blotting, sodium dodecyl sulfate–polyacrylamide gel electrophoresis sample buffer was added and the samples were heated for 5 min at 95 °C. In all, 20–40 μg of protein per lane were separated in sodium dodecyl sulfate–polyacrylamide gel electrophoresis mini gels and transferred to nitrocellulose membranes. The manufacturer's guidelines were followed for antibody hybridizations. ECL Western and ECL Advance

Western kits (Amersham, Little Chalfont, UK) were used for chemiluminescent signal detection.

Sequencing of complementary DNA and genomic DNA
Complementary DNA was prepared from Trizol (Invitrogen) extracted RNA, using M-MLV Reverse Transcriptase (Promega, Madison, WI, USA) and oligo dT(15) primers following the manufacturer's guidelines. Genomic DNA was extracted with the DNeasy Blood and Tissue kit (Qiagen, Hilden, Germany). Sequences of interest were amplified with gene specific primers and HotStar Taq Plus polymerase (Qiagen) following the manufacturer's protocol and gel purified. Gene-specific primers were used for DNA sequencing (Microsynth, Balgach, Switzerland).

AlamarBlue assay
In all, 10^4 cells per well were plated in 150 µl medium containing indicated concentrations of inhibitors in 96-well microtiter plates. Cells were grown for 42 h with inhibitors and labelled for 6 h at 37 °C with alamarBlue according to the manufacturer's protocols. Fluorescence was measured with a Safire Multiplate Reader (TECAN, Männedorf, Switzerland) and values were normalized to inhibitor-free and cell-free controls. S.D. were calculated using the mean value of three independent experiments, each performed in triplicate.

FACS analysis. For the viability assessment of cells, we performed FACS analysis after staining with 5 µg/ml PI in phosphate-buffered saline (Sigma-Aldrich) or Annexin V-FITC (Calbiochem, Darmstadt, Germany) following the manufacturer's guidelines. Plotting of the different fluorescence signals versus the side-scatter signal allowed gating and counting of cells.

siRNA treatment of human cells
For gene-specific knockdown we used siGENOME SMART Pools (Thermo Scientific Dharmacon, Rockford, IL, USA), controls were non-targeting siRNA and siDeath (Qiagen). siRNA pipetting was performed robotically. siRNA was diluted in OptiMEM (Gibco, Carlsbad, CA, USA) to 1 µM working dilution and stored at –20 °C. The transfection mix was prepared following the manufacturer's protocol with 8 µl of the siRNA working dilution mixed with 120 µl OptiMEM and 1.3 µl Lipofectamine RNAiMAX (Invitrogen). From this transfection mix, six transfections were carried out in parallel with each siRNA. Cells were trypsinized and allowed to adhere in 96-well microtiter plates filled with 150 µl medium before 20 µl of the transfection mix were added per well. Thus, a final concentration of 7 nM siRNA was used to transfect human fibroblasts (5000 cells per well), H1299 (5000 cells per well) or A549 (5000 cells per well). After 90 h, alamarBlue was added to three of the six plates and fluorescence was measured after 6 h incubation. The remaining three plates were trypsinized and cells stained with PI for FACS analysis. FACS profiles were imported to FlowJo 8.8.6 and PI-positive populations were gated, using the same gate per plate, including controls. AlamarBlue and PI values were imported to FileMaker Pro and the percentage of inhibition was normalized for each siRNA setting the actual value of the non-targeting siRNA to 0% and that of siDeath to 100% inhibition. This normalization allowed comparison of siRNA inhibition between different cell lines. A siRNA was considered inhibitory when the normalized mean of a PI-positive population was $>25\%$ and the difference between twice the standard error and twice the standard error of the non-targeting control was $>15\%$. In human fibroblasts, when this inhibitory threshold was reached, the siRNA was considered toxic. A toxicity threshold was also set if the mean alamarBlue fluorescence was below 50% of the non-targeting control siRNA with a minimal difference between the twice the standard errors of 35%.

Robotic screen
MISSION TRC shRNA lentiviral library containing around 80 000 individual clones representing around 15 000 genes was purchased from Sigma-Aldrich. Each clone contains a shRNA sequence and *puro* to select against non-infected cells. Each gene was targeted by at least three but normally five different clones. Minimal titer as specified by the supplier was 1×10^6 TFU/ml. The robotic screen was performed automatically using a BIOMEK-NX SYSTEM (Beckman-Coulter, Brea, CA, USA) with integrated multimode reader DTX880 and stacker carousel. The original library was in a 96-well format, from which a 1:5 working dilution with medium without IL-3 was made. Each of 930 plates was spiked with a non-targeting control virus (see above), and as positive control also with a Rictor targeting virus (see above). Four viral 96-well plates were transferred to one 384-well plate containing 3000 cells per well to a total volume of 30 µl giving a multiplicity of infection around 1. After 24 h incubation, plates were split into two parallel plates, to one of which saturating amounts of IL-3 was added. Puromycin (0.8 µg/ml) was added to all wells to remove non-infected cells. After further incubation for 3 days, alamarBlue was added, and after overnight incubation, growth was measured by determining fluorescence intensity (excitation: 560 nm; emission: 590 nm). Controls also included non-infected cells, which in the presence of puromycin were consistently negative. Spiking experiments with Rictor virus or control virus gave no false-positive/false-negative results (Supplementary Figure 2).

Data analysis of robotic screen
Proliferation data (alamarBlue fluorescence) were imported in FilemakerPro (Unterschleissheim, Germany). For each clone, the relative proliferation in presence and absence of IL-3 was calculated as a percentage of the respective values of a targeting virus versus that of the shControl virus, which was spiked on every 96-well plate. Dividing the relative proliferation in presence of IL-3 by the relative proliferation in the absence of IL-3 (rel. proliferation$_{+\mathrm{IL3}}$/rel. proliferation$_{-\mathrm{IL3}}$) gives the RI. A RI value of, for example, 5 corresponds to relative growth inhibition of 80%. In a paired analysis, the shRictor values from 800 plates were plotted. About 90% had an RI of >5 (data not shown). The number of false negatives can thus be estimated at being $<10\%$.

Quality control
Plates wherein the cells infected with shControl virus showed a relative proliferation below 25% in absence of IL-3 as compared with presence of IL-3 were eliminated and if possible repeated.

Functional analysis by Ingenuity software
Data were analyzed with Ingenuity Pathway Analysis (Ingenuity Systems). A data set of RI values from 13 407 genes were uploaded to Ingenuity, of which 12 599 were recognized. To eliminate off target effects, we restricted the analysis to genes in which at least two oligos had a RI of >5. When the mean RI of the three best oligos was set to a minimum of 7.3, 800 genes fulfilled these criteria and were eligible for network analysis. These genes are called group A genes.

For comparison, we also selected the top 800 genes whose knockdown inhibited proliferation of 6.5 cells both in the presence and absence of IL-3. In each case, the inhibition of proliferation relative to a control virus was $\geqslant 80\%$. This second group of genes was designated group 'B'. Group A and B genes were submitted to Canonical Pathway Analysis, which identified the pathways from the Ingenuity Pathways Analysis library that were most significant to the data set. Group A and B genes that were associated with a canonical pathway in the Ingenuity knowledge base were considered for the analysis. The significance of the association between the data set and the canonical pathway was measured in two ways: (1) a ratio of the number of genes from the data set that met the expression value cutoff that map to the pathway divided by the total number of molecules that exist in the canonical pathway is displayed. (2) Fischer's exact test was used to calculate a *P*-value determining the probability that the association between the genes in the data set and the canonical pathway is explained by chance alone.

Conflict of interest

CM is a consultant for Actelion Ltd.

Acknowledgements

We thank TW Sturgill for comments and Dr F Wenzel for providing normal human fibroblasts. We acknowledge support from the Commission of Technology and Innovation (CTI) (CM, MNH and UR), the Swiss National Science Foundation (CM and MNH) and the Swiss Cancer League and the Louis-Jeantet Foundation (MNH).

References

Alto NM, Soderling J, Scott JD. (2002). Rab32 is an A-kinase anchoring protein and participates in mitochondrial dynamics. *J Cell Biol* **158**: 659–668.

Bandyopadhyay G, Sajan MP, Kanoh Y, Standaert ML, Quon MJ, Reed BC *et al*. (2001). Glucose activates protein kinase C-zeta/lambda through proline-rich tyrosine kinase-2, extracellular signal-regulated kinase, and phospholipase D: a novel mechanism for activating glucose transporter translocation. *J Biol Chem* **276**: 35537–35545.

Bauer DE, Harris MH, Plas DR, Lum JJ, Hammerman PS, Rathmell JC *et al*. (2004). Cytokine stimulation of aerobic glycolysis in hematopoietic cells exceeds proliferative demand. *FASEB J* **18**: 1303–1305.

Bentzinger CF, Romanino K, Cloetta D, Lin S, Mascarenhas JB, Oliveri F *et al*. (2008). Skeletal muscle-specific ablation of raptor, but not of rictor, causes metabolic changes and results in muscle dystrophy. *Cell Metab* **8**: 411–424.

Chiang GG, Abraham RT. (2007). Targeting the mTOR signaling network in cancer. *Trends Mol Med* **13**: 433–442.

Cunningham JT, Rodgers JT, Arlow DH, Vazquez F, Mootha VK, Puigserver P. (2007). mTOR controls mitochondrial oxidative function through a YY1-PGC-1alpha transcriptional complex. *Nature* **450**: 736–740.

Dang CV. (2010). p32 (C1QBP) and cancer cell metabolism: is the Warburg effect a lot of hot air? *Mol Cell Biol* **30**: 1300–1302.

Fan Y, Dickman KG, Zong WX. (2010). Akt and c-Myc differentially activate cellular metabolic programs and prime cells to bioenergetic inhibition. *J Biol Chem* **285**: 7324–7333.

Fantin VR, Leder P. (2006). Mitochondriotoxic compounds for cancer therapy. *Oncogene* **25**: 4787–4797.

Foster DA. (2007). Regulation of mTOR by phosphatidic acid? *Cancer Res* **67**: 1–4.

Gandre-Babbe S, van der Bliek AM. (2008). The novel tail-anchored membrane protein Mff controls mitochondrial and peroxisomal fission in mammalian cells. *Mol Biol Cell* **19**: 2402–2412.

Gonez LJ, Naselli G, Banakh I, Niwa H, Harrison LC. (2008). Pancreatic expression and mitochondrial localization of the progestin-adipoQ receptor PAQR10. *Mol Med* **14**: 697–704.

Grandori C, Mac J, Siebelt F, Ayer DE, Eisenman RN. (1996). Myc-Max heterodimers activate a DEAD box gene and interact with multiple E box-related sites *in vivo*. *EMBO J* **15**: 4344–4357.

Guertin DA, Sabatini DM. (2007). Defining the role of mTOR in cancer. *Cancer Cell* **12**: 9–22.

Heyward CA, Pettitt TR, Leney SE, Welsh GI, Tavare JM, Wakelam MJ. (2008). An intracellular motif of GLUT4 regulates fusion of GLUT4-containing vesicles. *BMC Cell Biol* **9**: 25.

Hill MM, Clark SF, Tucker DF, Birnbaum MJ, James DE, Macaulay SL. (1999). A role for protein kinase Bbeta/Akt2 in insulin-stimulated GLUT4 translocation in adipocytes. *Mol Cell Biol* **19**: 7771–7781.

Jung HC, Kim K. (2005). Identification of MYCBP as a beta-catenin/LEF-1 target using DNA microarray analysis. *Life Sci* **77**: 1249–1262.

Kiser KF, Colombi M, Moroni C. (2006). Isolation and characterization of dominant and recessive IL-3-independent hematopoietic transformants. *Oncogene* **25**: 6595–6603.

Lipscomb EA, Sarmiere PD, Freeman RS. (2001). SM-20 is a novel mitochondrial protein that causes caspase-dependent cell death in nerve growth factor-dependent neurons. *J Biol Chem* **276**: 5085–5092.

Luo B, Cheung HW, Subramanian A, Sharifnia T, Okamoto M, Yang X *et al*. (2008). Highly parallel identification of essential genes in cancer cells. *Proc Natl Acad Sci USA* **105**: 20380–20385.

Luo J, Emanuele MJ, Li D, Creighton CJ, Schlabach MR, Westbrook TF *et al*. (2009). A genome-wide RNAi screen identifies multiple synthetic lethal interactions with the Ras oncogene. *Cell* **137**: 835–848.

Majumder PK, Febbo PG, Bikoff R, Berger R, Xue Q, McMahon LM *et al*. (2004). mTOR inhibition reverses Akt-dependent prostate intraepithelial neoplasia through regulation of apoptotic and HIF-1-dependent pathways. *Nat Med* **10**: 594–601.

Moffat J, Grueneberg DA, Yang X, Kim SY, Kloepfer AM, Hinkle G *et al*. (2006). A lentiviral RNAi library for human and mouse genes applied to an arrayed viral high-content screen. *Cell* **124**: 1283–1298.

Muller BA. (2009). Imatinib and its successors–how modern chemistry has changed drug development. *Curr Pharm Des* **15**: 120–133.

Murray JT, Campbell DG, Morrice N, Auld GC, Shpiro N, Marquez R *et al*. (2004). Exploitation of KESTREL to identify NDRG family members as physiological substrates for SGK1 and GSK3. *Biochem J* **384**: 477–488.

Nair AP, Hirsch HH, Moroni C. (1992). Mast cells sensitive to v-H-ras transformation are hyperinducible for interleukin 3 expression and have lost tumor-suppressor activity. *Oncogene* **7**: 1963–1972.

Nilsson R, Schultz IJ, Pierce EL, Soltis KA, Naranuntarat A, Ward DM *et al*. (2009). Discovery of genes essential for heme biosynthesis through large-scale gene expression analysis. *Cell Metab* **10**: 119–130.

Pagliarini DJ, Calvo SE, Chang B, Sheth SA, Vafai SB, Ong SE *et al*. (2008). A mitochondrial protein compendium elucidates complex I disease biology. *Cell* **134**: 112–123.

Polak P, Cybulski N, Feige JN, Auwerx J, Ruegg MA, Hall MN. (2008). Adipose-specific knockout of raptor results in lean mice with enhanced mitochondrial respiration. *Cell Metab* **8**: 399–410.

Pytel D, Sliwinski T, Poplawski T, Ferriola D, Majsterek I. (2009). Tyrosine kinase blockers: new hope for successful cancer therapy. *Anticancer Agents Med Chem* **9**: 66–76.

Ramanathan A, Schreiber SL. (2009). Direct control of mitochondrial function by mTOR. *Proc Natl Acad Sci USA* **106**: 22229–22232.

Root DE, Hacohen N, Hahn WC, Lander ES, Sabatini DM. (2006). Genome-scale loss-of-function screening with a lentiviral RNAi library. *Nat Methods* **3**: 715–719.

Sato T, Nakashima A, Guo L, Coffman K, Tamanoi F. (2010). Single amino-acid changes that confer constitutive activation of mTOR are discovered in human cancer. *Oncogene* **29**: 2746–2752.

Schieke SM, Phillips D, McCoy Jr JP, Aponte AM, Shen RF, Balaban RS *et al*. (2006). The mammalian target of rapamycin (mTOR) pathway regulates mitochondrial oxygen consumption and oxidative capacity. *J Biol Chem* **281**: 27643–27652.

Schlabach MR, Luo J, Solimini NL, Hu G, Xu Q, Li MZ *et al*. (2008). Cancer proliferation gene discovery through functional genomics. *Science* **319**: 620–624.

Scholl C, Frohling S, Dunn IF, Schinzel AC, Barbie DA, Kim SY *et al*. (2009). Synthetic lethal interaction between oncogenic KRAS dependency and STK33 suppression in human cancer cells. *Cell* **137**: 821–834.

Solimini NL, Luo J, Elledge SJ. (2007). Non-oncogene addiction and the stress phenotype of cancer cells. *Cell* **130**: 986–988.

Soria JC, Lee HY, Lee JI, Wang L, Issa JP, Kemp BL *et al*. (2002). Lack of PTEN expression in non-small cell lung cancer could be related to promoter methylation. *Clin Cancer Res* **8**: 1178–1184.

Thaimattam R, Banerjee R, Miglani R, Iqbal J. (2007). Protein kinase inhibitors: structural insights into selectivity. *Curr Pharm Des* **13**: 2751–2765.

van de Wetering M, Oving I, Muncan V, Pon Fong MT, Brantjes H, van Leenen D *et al*. (2003). Specific inhibition of gene expression using a stably integrated, inducible small-interfering-RNA vector. *EMBO Rep* **4**: 609–615.

Wang Q, Somwar R, Bilan PJ, Liu Z, Jin J, Woodgett JR *et al*. (1999). Protein kinase B/Akt participates in GLUT4 translocation by insulin in L6 myoblasts. *Mol Cell Biol* **19**: 4008–4018.

Weinberg F, Chandel NS. (2009). Mitochondrial metabolism and cancer. *Ann NY Acad Sci* **1177**: 66–73.

Weinberg F, Hamanaka R, Wheaton WW, Weinberg S, Joseph J, Lopez M *et al*. (2010). Mitochondrial metabolism and ROS generation are essential for Kras-mediated tumorigenicity. *Proc Natl Acad Sci USA* **107**: 8788–8793.

Wise DR, DeBerardinis RJ, Mancuso A, Sayed N, Zhang XY, Pfeiffer HK *et al*. (2008). Myc regulates a transcriptional program that stimulates mitochondrial glutaminolysis and leads to glutamine addiction. *Proc Natl Acad Sci USA* **105**: 18782–18787.

Wittwer AJ, Wagner C. (1980). Identification of folate binding protein of mitochondria as dimethylglycine dehydrogenase. *Proc Natl Acad Sci USA* **77**: 4484–4488.

Wullschleger S, Loewith R, Hall MN. (2006). TOR signaling in growth and metabolism. *Cell* **124**: 471–484.

Supplementary Information accompanies the paper on the Oncogene website (http://www.nature.com/onc)